1460 Russian Chemical Bulletin, Vol. 47, No. 8, August, 1998

Synthesis and reactivity of metal-containing monomers

50.* Evolution of short-range surrounding of Fe atoms during thermal transformation of $[Fe_3O(OOCCH=CHCOOH)_6]OH \cdot 3H_2O$

A. T. Shuvaev,[a] A. S. Rozenberg,[b] G. I. Dzhardimalieva,[b] N. P. Ivleva,[b] V. G. Vlasenko,[a] T. I. Nedoseikina,[a] T. A. Lyubeznova,[a] I. E. Uflyand,[c] and A. D. Pomogailo[b]*

[a]Institute of Physics of Rostov State University,
194 prosp. Stachki, 344104 Rostov-on-Don, Russian Federation
[b]Institute of Chemical Physics in Chernogolovka, Russian Academy of Sciences,
142432 Chernogolovka, Moscow Region, Russian Federation.
Fax: +7 (096) 515 3588. E-mail: adpomog@icp.ac.ru
[c]Rostov State Pedagogical University,
33 ul. B. Sadovaya, 344082 Rostov-on-Don, Russian Federation

Thermal transformations of Fe^{III} maleate, $[Fe_3O(OOCCH=CHCOOH)_6]OH \cdot 3H_2O$ (1), in an autogenerated atmosphere and the change in the short-range surrounding of Fe atoms during thermolysis were studied. The thermal transformations of 1 are accompanied by the following processes: dehydration with simultaneous rearrangement of the ligand environment and formation of maleic acid, and polymerization of the rearranged monomer and its decarboxylation at high temperatures. In the initial stage of decarboxylation, the destruction of the metal-carboxylate Fe_3O complex occurs followed by the formation of the Fe—Fe bond (r = 0.246 nm). The oxidation of the Fe atoms is observed when the thermolysis duration increases.

Key words: thermal transformation, iron maleate, dehydration, solid-phase polymerization, EXAFS spectroscopy.

The study of thermal transformations of polynuclear metal complexes with unsaturated monocarboxylic acids[1—3] showed that the thermolysis of the complexes is accompanied by solid-phase polymerization of ligands, and then the polymer (copolymer) is decarboxylated at high temperatures to form nanoparticles of metals or their oxides.[4] In this connection, it was of interest to study thermolysis of polynuclear complexes of unsaturated dicarboxylic acids.

In this work, we studied thermal transformations of the metallocomplex monomer, iron(III) maleate $[Fe_3O(OOCCH=CHCOOH)_6]OH \cdot 3H_2O$ (1), and the change in the short-range surrounding of Fe atoms during thermolysis.

Experimental

Complex 1 was obtained by the exchange reaction of Fe^{III} hydroxide with excess maleic acid according to the previously described procedure.[5] Found (%): C, 29.7; H, 3.12; Fe, 17.9. $[Fe_3O(OOCH=CHCOOH)_6]OH \cdot 3H_2O$. Calculated (%): C, 30.49; H, 2.65; Fe, 17.74. Elemental analysis was performed by the organic microanalysis method and atomic-adsorption technique on a Saturn instrument.

Thermal analysis of samples 1 was performed within the 20—600 °C range on a C derivatograph (MOM, Hungary) in air (the velocity of temperature increase was 10 deg min^{-1}).

The kinetics of isothermal transformation of 1 in the autogenerated atmosphere (AGA) and static isothermal system was studied at 300—370 °C and $(m_0/V) \cdot 10^3 \approx 3.85$ g cm^{-3} (m_0 is the initial mass of the sample, and V is the volume of the reaction vessel) by gas release using a membrane null-manometer. The heated volume with an ampule of the substance under study was not greater than 0.05 V. At the end of experiment, the mass loss of the sample, the amount of gaseous products at room temperature, and the amount of products condensing at 77 K were determined.

The specific surfaces (S_{sp}/m^2 g^{-1}) of the starting samples and transformation products were determined from the low-temperature nitrogen adsorption.

IR absorption spectra of gaseous and condensed products were recorded on Specord IR-75 and Perkin—Elmer-325 spectrophotometers in the range of 400—4000 cm^{-1}; solid samples were prepared as pellets with KBr.

Mass spectral analysis of gaseous products of transformation was performed on an MS 3702 quadruple mass spectrometer. The mass spectrometric study of 1 from a water-alcohol solution was performed on a time-of-flight mass spectrometer of the mass-reflectron type with extraction of dissolved ions at an atmospheric pressure (EDIAP).[6—8]

Specific features of short-range surrounding of Fe atoms in 1 and products of its thermal decomposition were studied by EXAFS spectroscopy on a laboratory EXAFS spectrometer created[9] on the basis of a DRON-3 diffractometer.

---

* For Part 49, see *Izv. Akad. Nauk, Ser. Khim.*, 1998, 1145 [*Russ. Chem. Bull.*, 1998, 47, 1113 (Engl. Transl.)].

Translated from *Izvestiya Akademii Nauk. Seriya Khimicheskaya*, No. 8, pp. 1505—1510, August, 1998.

A BSV-21-Mo tube served as the source of X-ray radiation. The radiation was decomposed to the spectrum by a quartz crystal-monochromator. The energy resolution in the region of the K-edge of the Fe absorption was 3 eV. Fe_2O_3 and $Fe(acac)_3$ were used as standards. The procedures of processing of EXAFS data were similar to those presented in Ref. 10. The accuracy of the method in determination of interatomic distances was ~0.002 nm.

Results and Discussion

Peculiarities of structure of complex 1. Complex **1** is a related polynuclear compound of the $[Fe_3OR_6 \cdot 3L]S$ type (here R is the anion of organic acid, and S is the molecule or anion that is not coordinated with the Fe atom), whose structures are well studied.[11,12] According to these data, the model of the structure of the nearest surrounding (MSNS) of the Fe atom in **1** can be presented as follows. The Fe atoms form a triangle with the Fe—Fe distance of ~0.33±0.003 nm,[11,12] in whose center the O atom coordinated to the Fe atoms is located (the Fe—O distance in the Fe—O—Fe bridge of the Fe_3 triangle is ~0.19 nm). In addition, each Fe atom is coordinated with the O atoms of the bidentate maleate groups R and the O atom of the H_2O molecule. Thus, the coordination number of the Fe atom in **1** is equal to 6.

The IR absorption spectrum of **1** contains, along with absorption bands (ν/cm^{-1}) of $\nu_{as}(COO^-)$ (1592 (br.s)), $\nu_s(COO^-)$ (1444 (s), 1399 (m), 1366 (m)) (characteristic of stretching vibrations of the bidentate-coordinated carboxyl group[13]), and ν(O—H) 3405 (br.m) (stretching vibrations of O—H of molecules of water of crystallization), an absorption related to ν_{COOH} 1700 (s) indicating the presence of COOH fragments in **1**.

In order to elucidate the peculiarities of the short-range surrounding of the Fe atoms in **1**, the original sample (**1a**) was studied by EXAFS spectroscopy.*

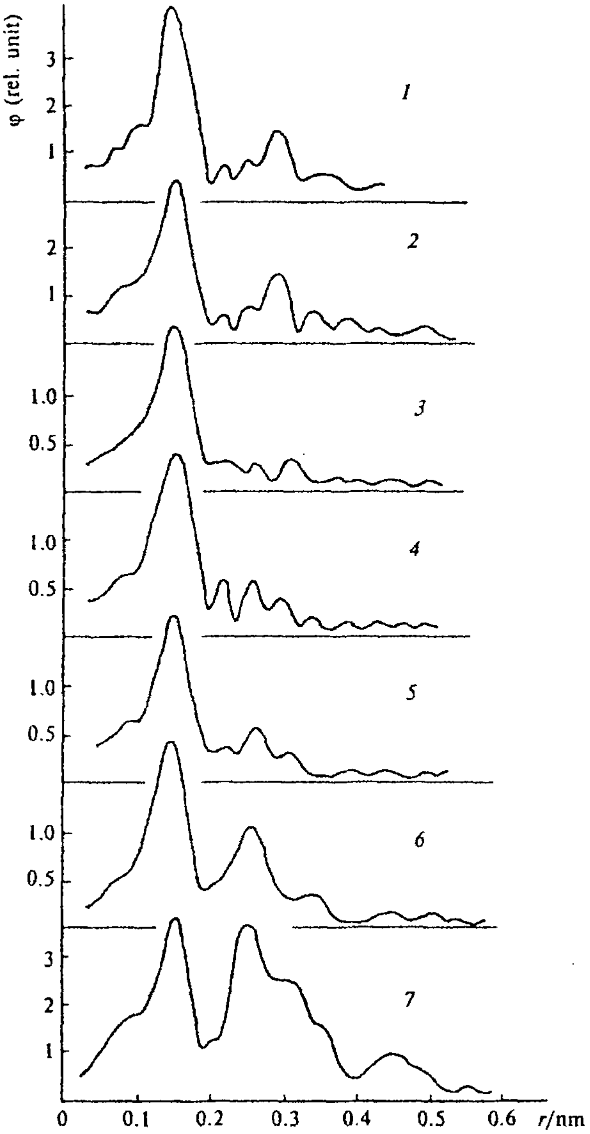

Fig. 1. Modulus of Fourier transformation of the EXAFS spectrum of the K-edge of Fe absorption: *1*, $Fe(acac)_3$; *2*, **1a**; *3*, **1b**; *4*, **1c**; *5*, **1d**; *6*, **1e**; and *7*, Fe_2O_3 (samples **1b**—**e** are products of isothermal thermolysis (370 °C) of **1** during 5, 7, 22, and 95 min, respectively).

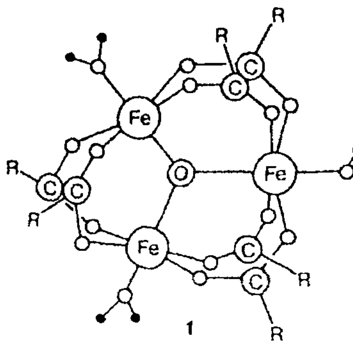

1

O — O
• — H
R = CH=CHCOOH

---

* The method is based on the phenomenon of photoelectron diffraction on atoms of the environment absorbing X-ray beams of the atom, which appears as a long-range fine structure of the X-ray absorption spectrum (EXAFS) of the chosen atom. Isolating the oscillating part of EXAFS and processing it by the Fourier transformation, one can obtain the modulus of Fourier transform (MFT), which represents (with an accuracy to phase corrections) a function of radial distribution of atoms in the surroundings of the absorbing atom. The position (r) of MFT maxima corresponds, as a rule, to radii R of coordination spheres (CS) ($R = r + \alpha$, where α is the phase correction), and their amplitudes are proportional to coordination numbers (N). The proportionality coefficient and α value are determined by analysis of EXAFS data of appropriate standard compounds with the known structures. In addition, R, N, and σ^2 values (thermal dispersion of the interatomic distance, the Debye—Waller factor) can be determined by the selection of values providing a good agreement between calculated and experimentally determined functions of the oscillating part of EXAFS (fitting method).

Table 1. MFT parameters for the nearest CS of the Fe atom in sample **1a**, products of its thermolysis (**1b—e**), and standard compounds

Compound	Number of CS (j)	MFT parameters		Structural data				CS
		r_j/nm	$\varphi_j \cdot 10^3$/nm^{-3}	R_j/nm [a]	N_j [a]	σ_j^2/nm^2	Q (%) [b]	
Fe(acac)$_3$	*1*	0.147	3.6	0.202 (0.200)	6.0 (6.0)	0.27	2	Fe—O
	—	0.216	0.6	—	—	—		s.m.[c]
	2	0.254	0.6	(0.295)	(5.4)	—		Fe—C
	3	0.292	1.2	(0.333)	(4.2)	—		Fe—C
1a	*1*	0.149	3.4	0.203 0.194	5.0 1.0	0.22 0.33	1.7	Fe—O Fe—O[d]
	—	0.217	0.5	—	—	—		s.m.[c]
	2	0.257	0.6	0.294	2.0	0.13		Fe—C
	3	0.293	1.2	0.329	2.0	0.23		Fe—Fe
1b	*1*	0.152	1.5	0.205	2.5	0.53	1.2	Fe—O
	—	0.217	0.3	—	—	—		s.m.[c]
	2	0.267	0.2	0.297				
1c	*1*	0.150	1.5	0.204	3.0	0.67	1.7	Fe—O
	2[e]	0.219	0.5	0.246	0.3	0.31	2.2	Fe—Fe +s.m.[c]
	2	0.262	0.4	0.292				Fe—Fe
1d	*1*	0.148	1.6	0.203	3.0	0.70	2.5	Fe—O
	—	0.225	0.3	—	—	—		s.m.[c]
	2	0.266	0.5	0.296				Fe—Fe
1e	*1*	0.147	1.9	0.199	4.0	0.74	0.9	Fe—O
	—	0.213	0.3	—	—	—		s.m.[c]
	2	0.264	1.1	0.294				Fe—Fe
Fe$_2$O$_3$	*1*	0.149	2.1	(0.196) (0.208)	3.0 3.0	— —		Fe—O Fe—O
	2	0.261	2.1	(0.287) (0.296)	1.0 3.0	— —		Fe—Fe Fe—Fe

[a] The data[14] of X-ray diffraction studies are given in parentheses.
[b] Q are the values of the target function characterizing the fitting accuracy.
[c] Secondary maximum.
[d] The distance from Fe to μ-O (bridging O atom) is indicated.
[e] The peak consists of CS of Fe—Fe and secondary maximum (s.m.) of the first CS.

The MFT obtained from the EXAFS spectra of the K-edge of the absorption of Fe for sample **1a** and standard compounds* are presented in Fig. 1 (spectra *2*, *1*, and *7*, respectively). The MFT parameters of the EXAFS spectra of the compounds studied are given in Table 1.

It is seen in Table 1 that the values of interatomic Fe—O distances in Fe(acac)$_3$ obtained in this work and previously[14] coincide within the error of the method. The φ_{st}, R_{st}, and N_{st} values for this standard compound can be used for the determination of R_j values using phase corrections α_j and N_j in the compounds studied, which can serve as the starting values in nonlinear fitting of model EXAFS spectra to experimental spectra.

Based on the above presented MSNS of Fe atoms, for the first CS of sample **1a**, we performed nonlinear fitting of the parameters of the calculated EXAFS signal and the signal separated from the experimental EXAFS spectrum by the Fourier filtration method of MFT[10] in the range of wave vectors of 0.115—0.26 nm^{-1}. The nonlinear fitting was performed by the Powel method of conjugated directions within the range of wave vectors k* from 27 to 118 nm^{-1}. The least Q value (the best fitting) was obtained for two-sphere fitting for the model with one bridging and five O atoms of ligands. The corresponding

---

* Iron acetylacetonate Fe(acac)$_3$ and Fe$_2$O$_3$ were chosen as standard compounds, because their atomic structures are well known and the nearest environment of the Fe atom in these compounds consists of O atoms as in sample **1a**. This allows one to find the values of phase shifts α_j and amplitudes φ_j for the corresponding CS of Fe—O and Fe—Fe from MFT of EXAFS spectra of the standard compounds and to use these values for determining R_j and N_j (j is the number of CS).

* The published[9] values of scattering amplitudes and phases of the photoelectron wave were used for fitting.

distances to the bridging O atom ($R_1' = 0.194$ nm) and O atoms of the ligands ($R_1 = 0.203$ nm) are close to the values obtained from the X-ray diffraction data[15] for $[Fe_3O(OOCMe)_6(py)_3](py)$ ($R_1' = 0.1909$ nm, $R_1 = 0.2064$, 0.2078 nm). The validity of the chosen MSNS of the Fe atom in sample **1a** should be confirmed by the appearance in MFT of a peak related to the Fe—Fe distance in the triangle fragment ($R_3 \approx 0.33$ nm). In fact, in MFT of the EXAFS spectrum, this peak occurs at $r_3 = 0.293$ nm. However, as can be seen in Table 1, the peak with these r_3 and φ_3 values is also present in MFT of $Fe(acac)_3$, where it unambiguously corresponds to the distance only to the C atoms of the ligands. The following procedure was used to prove the existence of CS consisting of Fe atoms in **1a**. It is known[10] that an increase in the lower integration limit in the Fourier analysis (k_{min}) from 25 to 60 nm^{-1} (taking into account predominantly high-energy photoelectrons) makes it possible to separate CS consisting of atoms with great atomic numbers. The φ_i/φ_1 value increases for CS with heavy atoms and remains almost unchanged for CS of light atoms. In our case, φ_i/φ_1 for sample **1a** increases by 2.3 times, whereas its increase is 1.2-fold for $Fe(acac)_3$. Thus, it can be asserted that the peak with $r = 0.293$ nm in MFT of **1a** corresponds to CS containing Fe atoms. According to the data of fitting, the corresponding Fe—Fe distance has the value $R_3 = 0.329$ nm; $N_3 = 2$. A similar distance is observed in $[Fe_3O(OOCMe)_6(py)_3](py)$ taken for comparison: according to the X-ray diffraction data,[15] $R = 0.3287$, 0.3279, and 0.3332 nm, *i.e.*, they are very close to the value obtained for **1a**. It follows from the results of fitting for CS with $r_2 = 0.257$ nm that it consists of approximately two atoms with a small atomic number. According to the model chosen, we assigned CS to the sphere consisting of C atoms of the maleate ligand.

Kinetic regularities of thermal transformation of complex 1. The study of **1** in the thermal analysis regime (Fig. 2) showed the following facts. The DTG curve (see Fig. 2, curve *3*) has four regions of the maximum rate of mass loss by the sample at 160, 245, 295, and 380 °C. The mass losses (Δm (wt.%)) are 31.25, 8.75, 6.25, and 25.0, respectively. The mass loss in the first region accompanied by sufficiently strong endoeffects at 140 and 160 °C (see Fig. 2, curve *1*) is related to both the dehydration process (5.2% for the loss of three water molecules) and, most likely, partial desolvation of three molecules of maleic acid (36.8% is the calculation for complete desolvation). The weak endoeffect accompanying the mass loss in the second region is most likely caused by polymerization of the desolvated monomer. As a rule, in these regions Δm is ~40%, which is close to the loss of three water molecules and three molecules of maleic acid (42% is the calculation). The mass loss in the regions of 295 and 380 °C is most likely related to decarboxylation of the polymer formed: 27.9% for the loss of six CO_2 molecules (calculation). Thus, at this moment Δm is 71.25% (71.36% is the calculation).

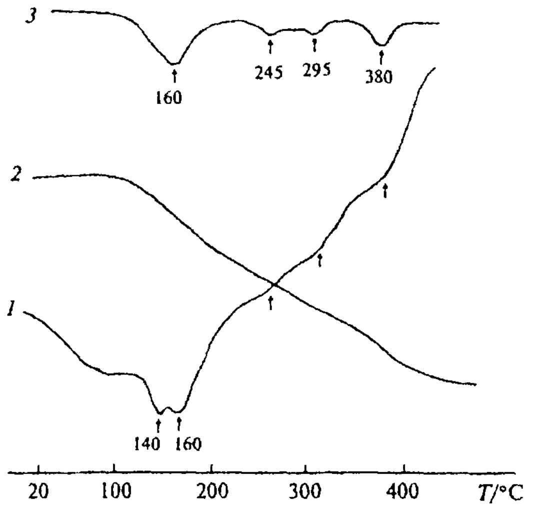

Fig. 2. Thermal analysis data for **1**: *1*, DTA; *2*, TG; and *3*, DTG ($m_0 = 64.0 \cdot 10^{-3}$ g).

The thermolysis of **1** is accompanied by gas release, and under isothermal conditions the main gas release is observed at $T_{exp} = 300$—370 °C. The gas release during heating of the sample to T_{exp} (~3—5 min) is almost independent of T_{exp}, and $\alpha^{\Sigma}_0 \approx 2.65\pm0.20$, where α^{Σ}_0 is the total number of moles of gaseous products released per mole of the starting substance during heating. The dependence of the gas release depth (η) on the time of thermolysis is satisfactorily approximated by the equation

$$\eta(t) = \eta_{1\infty}[1 - \exp(-k_1\tau)] + (1 - \eta_{1\infty})[1 - \exp(-k_2\tau)],$$

where $\eta = (\alpha^{\Sigma}_t - \alpha^{\Sigma}_0)/(\alpha^{\Sigma}_\infty - \alpha^{\Sigma}_0)$ is the conversion extent; α^{Σ}_t and α^{Σ}_∞ are the current and final amounts of α^{Σ}, respectively; $\tau = t - t_0$ (t_0 is the time of heating); and k is the effective rate constant. The values of k_1 and k_2 depend on T_{exp}: $k_1 = 3.3 \cdot 10^7 \exp[-(32000\pm2000)/(RT)]$, s^{-1}, $k_2 = 1.0 \cdot 10^7 \exp[-(26500\pm1900)/(RT)]$, s^{-1} (all activation energies are given in cal mol^{-1}). The $\eta_{1\infty}$ value increases as T_{exp} increases: $\eta_{1\infty} = 0.59 \cdot 10^2\exp[-5600/(RT)]$ (300—370 °C). It is noteworthy that, first, in the temperature range studied, k_1 exceeds k_2 by 2.5—3 times; second (which is remarkable), the values of activation parameters of k_1 are close to those (in this T_{exp} region) of the rate constants of decomposition of $[Fe_3O(CH_2CHCOOH)_6]OH \cdot 3H_2O$ [1] ($k = 1.3 \cdot 10^6\exp[-(30500\pm2000)/(RT)]$, s^{-1}) and its cocrystallizates with cobalt acrylate:[2] $k = 6.0 \cdot 10^6 \exp[-(33000\pm2000)/(RT)]$, s^{-1} (the Fe : Co atomic ratio is close to 1 : 0.8); $k = 6.6 \cdot 10^5 \exp[-(30000\pm2000)/(RT)]$, s^{-1} (2 : 1). The m_0/V ratio has no effect on the kinetics of thermal transformation in the temperature range studied.

Products of thermolysis of complex 1. The overall gas release at the end of the thermal transformation of **1** in the studied temperature range is greater than 4 mol and increases as T_{exp} increases from 4.78 (300 °C) to 7.40 (370 °C). According to the data of IR spectroscopy and mass spectrometry, CO_2 is the main gaseous product; CO is formed in an amount an order of magnitude lower than that of CO_2 ($\leq$10% of the amount of CO_2), and H_2 is released in trace amounts. The yield of CO_2 (α_{CO_2}) at the end of gas release increases as T_{exp} increases from 4.29 (300 °C) to 6.73 (370 °C). The yield of CO (α_{CO}) also increases with T_{exp} increase from 0.22 (300 °C) to 0.53 (370 °C). It is remarkable that at high temperatures (>360 °C) the value of $\alpha_{CO_2} + \alpha_{CO}$ exceeds 6.0, which could be expected for decarboxylation of six metallocarboxylate groups of the maleate ligand. In addition to CO_2, CO, and H_2, the gaseous products contain H_2O vapor, which is condensed on the "cool" (T_{room}) parts of the reaction vessel. Simultaneously, during heating of the sample, maleic acid is crystallized on the "cool" parts of the reaction vessel, which is confirmed by the comparison of the IR absorption spectra of the condensate and maleic acid.

The level of mass loss by the sample at the end of gas release increases with the T_{exp} increase from 48.15 (300 °C) to 57.1 wt.% (370 °C). During thermolysis at the T_{exp} studied, Δm changes very unusually. The main mass loss is observed during heating to T_{exp}. For example, at T_{exp} = 350 °C Δm is 46.3 wt.%, *i.e.*, it exceeds 42% expected for the loss by **1** of three water molecules and three molecules of maleic acid, which is related to the release of CO due to decarboxylation. In the further gas release, the rate of the Δm increase decreases substantially, and at the end of the process Δm reaches 57—58 wt.%, which is lower than the values observed in the thermoanalytical studies (71.25 wt.%).

Compound **1** readily loses three water molecules and three molecules of maleic acid, which is also indicated by the results of the mass spectrometric study of **1** by the EDIAP method. The peak in the mass spectrum with the maximum *m/z* value (Fig. 3) corresponds to the $[Fe_3O(OOCH{=}CHCOO)_3]^+$ ion (*m/z* = 525.5). This fact suggests that already during dissolvation, monomer **1** rather readily loses three molecules of maleic acid and three molecules of water of crystallization, and the O atoms of the maleate anion of both carboxylate groups are coordinated around the Fe atoms.

Change in short-range surrounding of Fe atoms during transformation of complex 1. The EXAFS study was performed for solid-phase products of the transformation of **1** under isothermal conditions at 370 °C and different thermolysis durations (t_{term} = 5, 7, 22, and 95 min), which corresponded to the pressure of released gaseous products p^{Σ} = 265, 303, 400, and 500 Torr. The mass losses by the sample were the following (wt.%): 46.8 (depth with respect to gas release $\eta_{\Delta\alpha}$ = 0.50, sample **1b**), 48.2 (0.57, **1c**), 54.25 (0.745, **1d**), and 57.1 (1.0, **1e**), respectively. The MFT obtained from the EXAFS spectra of the K-edge of the Fe absorption and their parameters for **1b**—**e** are presented in Fig. 1 and Table 1, respectively.

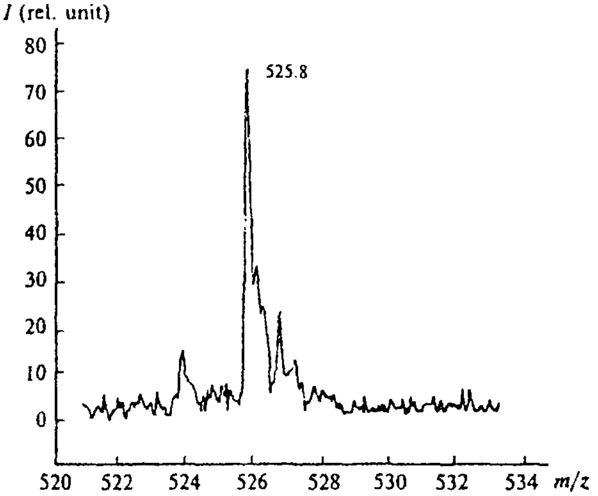

Fig. 3. Mass spectrum of the molecular cation $[Fe_3O(OOCH{=}CHCOO)_3]^+$ at the voltage of 260 V.

It is noteworthy for examination of changes in the short-range surrounding of Fe atoms during thermolysis of **1** that sample **1b** is in fact the result of the following transformations of **1** during heating: loss of three water molecules and three molecules of maleic acid; polymerization and the initial stage of decarboxylation of the polymer formed.

As can be seen from the data in Table 1, the amplitude of the peak of MFT of the EXAFS spectra of **1b**—**d** corresponding to the first coordination sphere is halved as compared to the value for **1a**. The calculated mean coordination number for these samples $N_1 \approx 3$. The R_1 distance for Fe—O decreases from 0.205 to 0.199 nm on going from **1b** to **1e**. It is known[1,2,16,17] that annealing of complexes and metallopolymers often results in the formation of ultradispersed particles of different types: metal clusters, oxides, carbides, *etc.* Under certain regimes of annealing, the complexes can lose ligands (or decompose) to form metal—metal bonds, for example, in the form of dimers.[17] In the case of the formation of these bonds during the transformation of **1**, the peak with $r \approx$ 0.21—0.22 nm corresponding to the distance for the direct metal—metal interaction (in α-Fe R = 0.248 nm) should appear in the MFT of the EXAFS spectra of samples **1b**—**e**. However, the secondary maximum of the first CS has the same *r* values in MFT, which requires one to develop a procedure of separation of superposing peaks. We used the fact that the appearance of the secondary maximum (s.m.) is related to the specific features of the Fourier transformation in which each CS has, along with the main maximum, s.m. with a small amplitude remote at a certain distance from the main peak, and the amplitude of the secondary peak is a certain fraction of the amplitude of the main peak. For the experimental determination of the amplitude of s.m., we used MFT of the EXAFS spectrum of the standard $Fe(acac)_3$ sample without metal—metal inter-

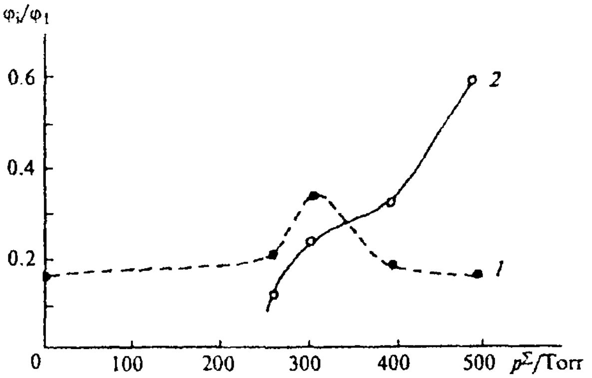

Fig. 4. Dependences of $\varphi_{s.m.}/\varphi_1$ on the pressure of gaseous products (p^{Σ}) released during thermolysis (samples **1a—e**): *1*, j = s.m.; *2*, j = 2.

action. The amplitude of s.m. ($\varphi_{s.m.}$) was ~17% of the amplitude of the main peak. The $\varphi_{s.m.}/\varphi_1$ dependences on the pressure of the released gaseous products for samples **1a—e** are presented in Fig. 4 and show that the amplitudes of the peaks with $r \approx 0.213$—0.22 nm in MFT of **1a—e** are almost equal to the amplitude of s.m., *i.e.*, these peaks contain no contributions from CS of Fe atoms. However, for sample **1c**, the amplitude of this peak is twice as much and, hence, this contribution takes place. The two-sphere fitting made it possible to determine the corresponding distance of $r = 0.246$ nm, which is close to the Fe—Fe distance in bulky metal (α-Fe, 0.248 nm).

A systematic increase in the amplitude of the peak with $r \approx 0.264$ nm during thermolysis (see Fig. 4, curve *2*) is another specific feature of MFT of samples **1b—f**. The comparison of the EXAFS spectra and parameters of MFT of sample **1e** and Fe_2O_3 suggests that this peak is characteristic of Fe oxide, and its behavior indicates that Fe atoms are oxidized as the thermolysis duration increases. The reaction

$$FeO_x + y\,CO_2 = FeO_{x+z} + (y - z)\,CO_2 + z\,CO$$

is most likely one of the routes of formation of Fe oxides, which is indicated by an increase in the yield of CO during the transformation: 0 (t_{term} = 5 min), 0.12 (7), 0.23 (22), and 0.53 (95).

Thus, the thermal transformation of **1** is related to the following processes: dehydration with the simultaneous rearrangement of the ligand environment accompanied by the formation of maleic acid; polymerization of the rearranged monomer and its decarboxylation at high temperatures. At the initial stage of decarboxylation, the polynuclear metal-carboxylate complex $[Fe_3OR_6]$ (sample **1b**) is destroyed to form most likely Fe—Fe bonds (sample **1c**). As the thermolysis duration increases, the Fe atoms are oxidized.

This work was financially supported in part by the Russian Foundation for Basic Research (Project No. 98-03-32353a).

References

1. A. S. Rozenberg, E. I. Aleksandrova, G. I. Dzhardimalieva, A. N. Titkov, and A. D. Pomogailo, *Izv. Akad. Nauk, Ser. Khim.*, 1993, 1743 [*Russ. Chem. Bull.*, 1993, **42**, 1666 (Engl. Transl.)].
2. A. S. Rozenberg, E. I. Aleksandrova, G. I. Dzhardimalieva, N. V. Kir'yakov, P. E. Chizhov, V. I. Petinov, and A. D. Pomogailo, *Izv. Akad. Nauk, Ser. Khim.*, 1995, 885 [*Russ. Chem. Bull.*, 1995, **44**, 858 (Engl. Transl.)].
3. A. S. Rozenberg, E. I. Aleksandrova, G. I. Dzhardimalieva, and A. D. Pomogailo, *Izv. Akad. Nauk, Ser. Khim.*, 1993, 303 [*Russ. Chem. Bull.*, 1993, **42**, 259 (Engl. Transl.)].
4. A. S. Rozenberg, G. I. Dzhardimalieva, and A. D. Pomogailo, *Dokl. Akad. Nauk*, 1997, **356**, 66 [*Dokl. Chem.*, 1997 (Engl. Transl.)].
5. N. P. Porollo, Z. G. Aliev, G. I. Dzhardimalieva, I. N. Ivleva, I. E. Uflyand, A. D. Pomogailo, and N. S. Ovanesyan, *Izv. Akad. Nauk, Ser. Khim.*, 1997, 375 [*Russ. Chem. Bull.*, 1997, **46**, 362 (Engl. Transl.)].
6. *Byul. Izobr.* [*Invention Bull.*], 1991, No. 36 (in Russian).
7. I. V. Chernushevich, Ph. D. (Phys.-Math.) Thesis, Chernogolovka, 1991 (in Russian).
8. Yu. M. Shul'ga, O. S. Roshchupkina, G. I. Dzhardimalieva, I. V. Chernushevich, A. F. Dodonov, Yu. V. Baldokhin, P. Ya. Kolotyrkin, A. S. Rozenberg, and A. D. Pomogailo, *Izv. Akad. Nauk, Ser. Khim.*, 1993, 1739 [*Russ. Chem. Bull.*, 1993, **42**, 1661 (Engl. Transl.)].
9. A. T. Shuvaev, B. Yu. Khal'mer, and T. A. Lyubeznova, *Pribory i tekhnika eksperimenta* [*Instruments and Experimental Techniques*], 1988, 234 (in Russian).
10. D. I. Kochubei, Yu. A. Babanov, K. I. Zamaraev, R. V. Vedrinskii, V. L. Kraizman, G. N. Kulipanov, L. N. Mazalov, A. N. Skrinskii, V. K. Fedorov, B. Yu. Khel'mer, and A. T. Shuvaev, *Rentgenospektral'nyi metod izucheniya struktury amorfnykh tel: EXAFS-spektroskopiya* [*X-ray Spectral Method for Studying Amorphous Bodies: EXAFS Spectroscopy*], Nauka, Sibirskoe Otdelenie, Novosibirsk, 1988 (in Russian).
11. M. A. Porai-Koshits, in *Kristallokhimiya, Itogi nauki i tekhniki* [*Crystallochemistry, Advances in Science and Technology*], VINITI, Moscow, 1981, **15**, 13 (in Russian).
12. S. M. Oh, S. R. Wilson, D. N. Hendrickson, S. E. Woehler, R. J. Wittebort, D. Inniss, and C. E. Strouse, *J. Am. Chem. Soc.*, 1987, **109**, 1073.
13. K. Nakamoto, *Infrared and Raman Spectra of Inorganic and Coordination Compounds*, Wiley and Sons, New York, 1987.
14. R. C. Scarrow, M. J. Maroney, S. M. Palmer, L. Jr. Que, A. L. Roe, S. P. Salowe, and J. Stubbe, *J. Am. Chem. Soc.*, 1987, **109**, 7857.
15. B.-K. Teo and P. A. Lee, *J. Am. Chem. Soc.*, 1979, **101**, 7215.
16. A. V. Kozinkin, V. G. Vlasenko, A. T. Shuvaev, S. P. Gubin, I. A. Dubovtsev, *Izv. Akad. Nauk, Neorg. Soedin.*, 1996, 32, 422 [*Inorg. Mater.*, 1996, **32** (Engl. Transl.)].
17. V. G. Vlasenko, F. M. Ovsyannikov, A. V. Kozinkin, A. T. Shuvaev, L. M. Bronshtein, and P. M. Valetskii, *Vysokomol. Soedin., Ser. A and B*, 1995, 37, 1414 [*Polym. Sci. USSR*, 1995, **37** (Engl. Transl.)].

Received November 25, 1997